Effect of Spacer Length on the Thermal Properties of Side-Chain Liquid Crystal Polymethacrylates. 2.† Synthesis and Characterization of the Poly[ω-(4′-cyanobiphenyl-4-yloxy)alkyl methacrylate]s

Aileen A. Craig and Corrie T. Imrie*

Department of Chemistry, University of Aberdeen, Meston Walk, Old Aberdeen, AB9 2UE, Scotland

Received December 27, 1994; Revised Manuscript Received February 28, 1995®

ABSTRACT: A new homologous series of side-chain liquid crystal polymers, the poly[ω-(4′-cyanobiphenyl-4-yloxy)alkyl methacrylate]s, has been synthesized in which the spacer length is varied from 3 to 12 methylene units. The thermal behavior of the polymers has been characterized using differential scanning calorimetry and polarized light microscopy. The propyl homologue is amorphous while the remaining members of the series all exhibit liquid crystallinity, specifically smectic behavior. The glass transition temperatures decrease with a small odd–even effect before reaching a limiting value as the length of the spacer is increased. The clearing temperatures exhibit a more pronounced odd–even effect on increasing the spacer length. In both alternations the odd members exhibit the higher values. The molecular significance of the odd–even effect exhibited by the glass transition temperatures was unclear while that shown by the clearing temperatures was rationalized in terms of the change in the average shape of the side chains as the parity of the spacer is varied. The properties of this cyanobiphenyl-based series are compared to those of the analogous materials containing methoxybiphenyl, and differences are accounted for in terms of the local side-chain packing within the mesophase. The influence of backbone flexibility on liquid crystal properties of side-chain polymers is also considered, and this polymer series tends to support the view that increasing backbone flexibility increases the clearing temperature while decreasing the entropy change associated with the transition.

Introduction

Side-chain liquid crystal polymers continue to be the focus of much research interest. This intense activity pertains not only as a result of the considerable application potential of this class of polymers[1,2] but also because they provide a testing challenge to our understanding of the structural factors that promote liquid crystallinity in polymeric systems.[3,4] A side-chain liquid crystal polymer comprises three structural units: a polymer backbone, a flexible spacer, and a mesogenic core. The role of the flexible spacer is to decouple, to some extent, the relative tendencies of the mesogenic groups to self-assemble from those of the polymer backbone to adopt a random coil configuration and, hence, endows upon the polymer a duality of properties. Thus, side-chain liquid crystal polymers exhibit macromolecular characteristics, such as mechanical integrity, coupled with the electro-optic properties of low molar mass mesogens, albeit on a much slower time scale. This combination of properties has led to the proposed use of side-chain liquid crystal polymers in areas such as optical information storage[5] and nonlinear optics.[6] In order to design new materials having targeted properties for such applications, we must first develop and understand knowledge-based rules relating polymer structure to liquid crystal properties. Although there is now a wealth of data in the literature describing the liquid crystal properties of these materials,[3,4] there are surprisingly few studies in which the length and parity of the spacer is varied in a systematic fashion for a given backbone and mesogenic group. Such studies have been limited to poly(vinyl ether)s,[7–15] poly(norbornene)s,[16–18] and polystyrenes.[19–24] For each of these systems homologous series containing at least ten homologues have been reported. Most recently, we have described a synthetic methodology to allow the systematic variation of the length and parity of the spacer in polymethacrylate-based materials and incorporated methoxybiphenyl as the mesogenic group.[25] In order to investigate the generality of the relationships revealed in this study, we have now prepared the homologous series of polymers, the poly[ω-(4′-cyanobiphenyl-4-yloxy)alkyl methacrylate]s, in which the spacer

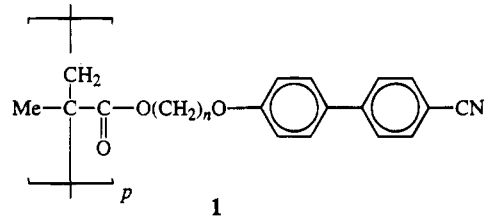

1

has been varied from three to twelve methylene units. The acronym PMA-*n* is used to refer to the polymers **1** in which *n* denotes the number of methylene groups in the flexible spacer. 4-Cyanobiphenyl has been used in this study because it is the most widely used mesogenic core and has been attached to a wide range of backbone types.[22] This allows the effect of backbone flexibility also to be considered.

Experimental Section

The polymers were prepared using the synthetic route shown in Scheme 1. Identical procedures were used to prepare all the members of series **2** and **3** (see Scheme 1), and hence only a representative description is given for the monomer synthesis.

Materials. α,ω-Dibromoalkanes (Aldrich) were distilled under reduced pressure using a Kugelrohr apparatus im-

† Part 1: Craig, A. A.; Imrie, C. T. *J. Mater. Chem.* **1994**, *4*, 1705.

* To whom correspondence should be addressed.

® Abstract published in *Advance ACS Abstracts,* April 1, 1995.

0024-9297/95/2228-3617$09.00/0

Scheme 1

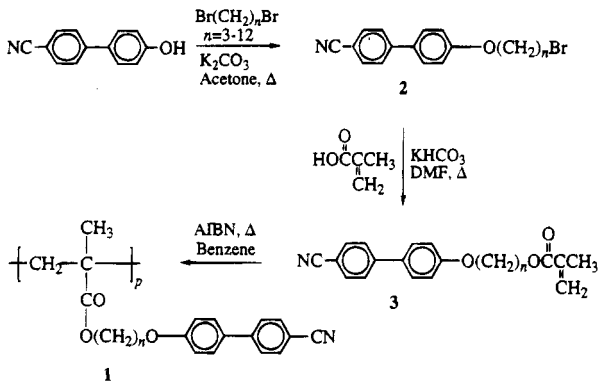

mediately prior to use. Benzene and tetrahydrofuran (THF) were distilled over calcium hydride. AIBN was purified by recrystallization from toluene, washed with petroleum spirits (80–100 °C) and dried under vacuum. 4-Hydroxy-4′-cyanobiphenyl, dry acetone, methacrylic acid, hydroquinone, and *N*,*N*-dimethylformamide were all used as received (Aldrich).

Monomer Synthesis. 1-Bromo-8-(4′-cyanobiphenyl-4-yloxy)octane (**2**) was prepared using a procedure described by Attard *et al.*[26] Thus, 4-hydroxy-4′-cyanobiphenyl (2.5 g, 13 mmol), 1,8-dibromooctane (23.9 mL, 130 mmol), and potassium carbonate (13.5 g, 97.5 mmol) were refluxed with stirring in dry acetone (200 mL) overnight. The reaction mixture was filtered hot, the residue washed with acetone, and the solvent removed under reduced pressure. Light petroleum (40–60 °C) was added to the extract, and the resulting precipitate was collected. The crude product was recrystallized twice from ethanol with hot filtration. This ensured the complete removal of any dimeric side product that may have formed during the reaction. Yield: 3.7 g, 73%. mp: 72.4–73.8 °C. IR (KBr) ν/cm^{-1}: 2224 (vs CN). ^{1}H NMR ($CDCl_3$): δ 7.7 (m, 4H, aromatic), 7.5 (m, 2H, aromatic), 7.0 (m, 2H, aromatic), 4.0 (t, 2H, *J* 6.5 Hz, OCH_2), 3.4 (t, 2H, *J* 6.8 Hz, CH_2Br), 1.7–2.0 (m, OCH_2CH_2, CH_2CH_2Br), 1.2–1.5 (m, 8H, $O(CH_2)_2(CH_2)_4(CH_2)_2$-Br).

8-(4-Cyanobiphenyl-4′-yloxy)octyl methacrylate (**3**) was prepared using a modification of the procedures described by Nakano *et al.*[27] and Shannon.[28] Methacrylic acid (0.66 g, 7.7 mmol) was stirred with potassium hydrogen carbonate (0.74 g, 7.4 mmol) for 5 min at room temperature to form the potassium methacrylate salt. This salt was added to **2** (2 g, 5.2 mmol) and hydroquinone (0.015 g, 0.14 mmol) in *N*,*N*-dimethylformamide (60 mL), and the reaction mixture was refluxed with stirring at 100 °C overnight. On cooling, the mixture was poured into water (*ca.* 300 mL) and stirred to coagulate the precipitate which was collected by filtration and dissolved in dichloromethane. The organic solution was washed with 5% aqueous sodium hydroxide and then water. The organic layer was dried over $MgSO_4$, and filtered, and the solvent was removed. The crude product was recrystallized twice from ethanol. Yield: 1.5 g, 74%. mp: 46.2–47.2 °C. IR (KBr) ν/cm^{-1}: 2223 (vs CN), 1701 (vs C=O), 1633 (C=C). ^{1}H NMR ($CDCl_3$): δ 7.7 (m, 4H, aromatic), 7.5 (m, 2H, aromatic), 7.0 (m, 2H, aromatic), 5.6, 6.1 (s, 2H, CH_2=C), 4.2 (t, 2H, *J* 6.7 Hz, $H_2COC(O)$), 4.0 (t, 2H, *J* 6.5 Hz, OCH_2), 2.0 (s, 3H, CH_3), 1.6–1.9 (m, 4H, OCH_2CH_2, $CH_2CH_2OC(O)$), 1.3–1.5 (m, 8H, $O(CH_2)_2(CH_2)_2(CH_2)_2C(O)$).

Polymerization. Monomer **3** (1 g) was dissolved in benzene (10 mL), and 1 mol % AIBN was added as initiator. The reaction mixture was flushed with argon for 20 min and placed in a water bath at 60 °C to initiate polymerization. After 48 h the reaction was terminated on addition of THF (15 mL) and the polymer precipitated into a large amount of methanol. The polymer was then redissolved into THF and reprecipitated into methanol. The removal of the alkene was monitored spectroscopically. The alkene stretch at 1633 cm^{-1} in the IR spectra of the monomers and the peaks associated with the alkene protons at 5.6 and 6.1 ppm in the ^{1}H NMR spectra were not present in those of the corresponding polymer. PMA-8: Yield: 0.75 g, 68%. IR (KBr) ν/cm^{-1}: 2225 (vs CN), 1728 (vs C=O). ^{1}H NMR (THF-d_8) δ 7.7 (m, 4H, aromatic), 7.5 (m, 2H, aromatic), 7.0 (m, 2H, aromatic), 3.8–4.0 (m, 4H, OCH_2), 1.2–2.0 (m, 14H, CH_2), 0.8–1.2 (m, 3H, CH_3).

Table 1. Molecular Weights and Thermal Properties of Polymers 1

n	M_n/g mol^{-1}	M_w/g mol^{-1}	PD	T_g/°C	T_{Cl}/°C	ΔH/kJ mol^{-1}	$\Delta S/R$
3	20 800	29 200	1.40	66			
4	19 500	28 100	1.44	57	99	0.61	0.19
5	16 700	26 500	1.59	63	112	2.09	0.65
6	20 300	33 700	1.66	24	98	1.84	0.59
7	28 100	45 900	1.64	30	116	3.06	0.95
8	25 100	42 600	1.70	18	109	2.35	0.74
9	35 700	68 900	1.93	23	121	3.29	1.01
10	35 800	67 500	1.89	12	101	3.45	1.11
11	31 600	47 000	1.49	16	120	3.97	1.22
12	34 000	63 000	1.85	11	117	4.16	1.28

Characterization. The proposed structures of all the compounds were verified using ^{1}H NMR and IR spectroscopy. ^{1}H NMR spectra were measured in $CDCl_3$ or THF-d_8 on a Bruker AC-F 250 MHz NMR spectrometer. IR spectra were recorded using a Nicolet 205 FTIR spectrometer. The purities of all the intermediates were verified using thin-layer chromatography. The molecular weights of the polymers were measured by gel permeation chromatography (GPC) using a Knauer Instruments chromatograph equipped with two PL Gel 10 μm mixed columns and controlled by Polymer Laboratories GPC SEC V5.1 software. THF was used as the eluent. A calibration curve was obtained using polystyrene standards.

The thermal properties of the polymers were determined by differential scanning calorimetry (DSC) using a Polymer Laboratories PL-DSC equipped with an autocool accessory and calibrated using an indium standard. Two samples were used for each polymer and the results averaged. The time–temperature profile for each was identical. Thus, each sample was heated from 25 to 230 °C, maintained at 230 °C for 3 min, cooled to −50 °C, maintained at −50 °C for 3 min, and finally reheated to 230 °C. The heating and cooling rate in all cases was 10 °C min^{-1}. The identification of liquid crystalline phases was performed by polarized light microscopy using an Olympus BH-2 optical microscope equipped with a Linkam THMS 600 heating stage and TMS 91 control unit. Clear, characteristic optical textures from which phase assignments were possible were obtained by cooling at either 0.2 or 0.1 °C min^{-1} from *ca.* 10 °C above the clearing temperature to below the glass transition temperature or, in the absence of glassy behavior, to room temperature.

Results and Discussion

The thermal properties, molecular weights, and polydispersities of the PMA-*n* series, **1**, are listed in Table 1. The number-average molecular weights of the polymers range from 16 700 to 35 800 g mol^{-1} with a corresponding degree of polymerization range of 48–88. These values are sufficiently high to ensure that the thermal properties of the polymers lie outside the molecular weight dependent regime,[23] allowing meaningful comparisons to be made of the thermal behavior of members within the series and with other polymers reported in the literature. The tacticities of the polymers were evaluated from their ^{1}H NMR spectra, and this revealed predominantly atactic materials with significant amounts of syndiotactic placements but a very small isotactic fraction. This analysis was only possible for polymers with short spacer lengths as the peak associated with $CH_2CH_2CH_2$ overlapped that arising from the backbone methyl groups in isotactic arrangements.

Figure 1 shows the second heating DSC trace for each polymer and from these the data listed in Table 1 were extracted. The propyl homologue, *i.e.*, PMA-3, did not exhibit liquid crystallinity. By contrast, the remaining members of the series all exhibit thermotropic liquid

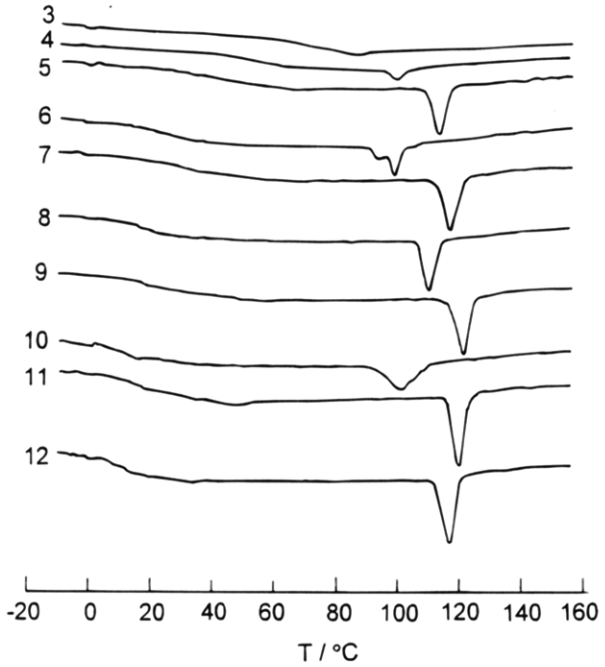

Figure 1. Normalized DSC traces obtained on the second heating of the PMA-*n* series.

crystal behavior. For PMA-4 a poorly defined focal conic fan texture was obtained indicative of a smectic phase. The associated entropy change, however, is somewhat smaller than that normally associated with a smectic–isotropic transition and is more typical of the value observed for nematic–isotropic transitions. For PMA-5 a clear characteristic focal conic fan texture is obtained and in consequence this is assigned as a smectic A phase. For PMA-6 a focal conic fan texture develops on cooling from the isotropic phase, but no further textural change is observed on cooling to temperatures below that corresponding to the shoulder on the endothermic peak in the DSC trace, see Figure 1. The higher temperature phase is assigned as a smectic A phase while the absence of any further textural changes suggests that the lower temperature phase may be either a crystal or smectic B phase. On cooling PMA-7, PMA-8, and PMA-9 from the isotropic phase, batonnets develop which coalesce, giving rise to a well-defined focal conic fan texture. This is assigned as a smectic A phase and the magnitude of the entropy changes associated with the clearing transition for each polymer support this view. On cooling PMA-10, a poorly defined focal conic fan texture was obtained. On cooling PMA-11 and PMA-12 from the isotropic phase, batonnets developed and coalesced to give a well-defined focal conic fan texture; see Figure 2; these are assigned as smectic A–isotropic transitions. On further cooling, however, continuous bands developed across the backs of the fans which persisted to room temperature; see Figure 3. The bands appeared at *ca.* 70 °C for both polymers. These changes are indicative of an E–smectic A phase transition.

The thermal properties of four members of the PMA-*n* series have been reported in the literature.[29–33] The ethyl homologue, PMA-2, is amorphous with a T_g at 95 °C. The behavior of PMA-5 reported here is in excellent agreement with that described in the literature. The clearing temperatures and associated entropy changes for PMA-6 and PMA-11 (see Table 1), are also in excellent agreement with the literature values. By contrast, the glass transition temperatures listed in Table 1 for these polymers are lower, by 31 and 24 °C,

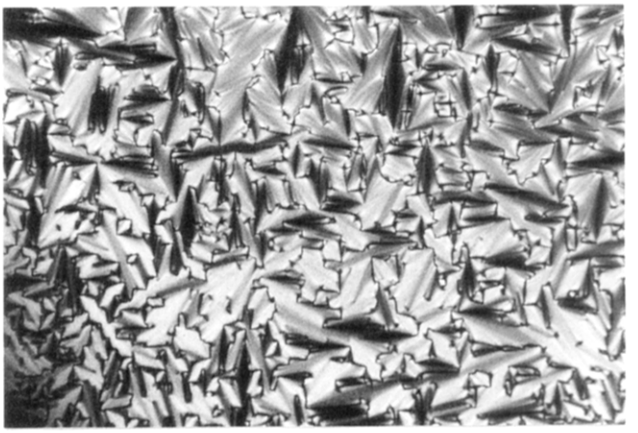

Figure 2. Focal conic fan texture exhibited by PMA-11 (T = 118 °C).

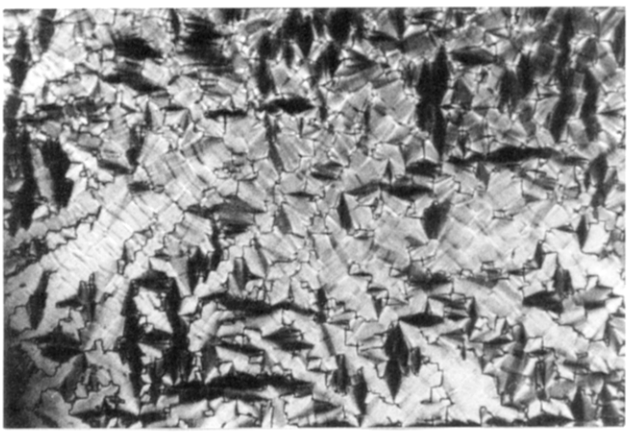

Figure 3. Arced focal conic fan texture obtained by cooling the preparation in Figure 2 (T = 27 °C).

respectively, than those reported elsewhere. These apparently serious discrepancies may be attributed to the use of different techniques for evaluating T_g; the values quoted here are extracted from DSC data whereas those in the literature were determined using a thermomechanical method.[31] The proposed phase assignments are also in agreement with those in the literature although the lower temperature phase exhibited by PMA-11 was not reported.[32] The smectic A phase exhibited by PMA-5 and PMA-11 was shown by X-ray diffraction to have an interdigitated structure.[32]

Figure 4 shows the dependence of the transition temperatures on the number of methylene groups n in the flexible alkyl spacer for the PMA-*n* series. The glass transition temperatures decrease initially with increasing chain length before reaching a limiting value at *ca.* 12 °C. Superimposed on this trend is a small but distinct odd–even effect with the odd members exhibiting the higher values. Similar behavior was observed for mesogenic polystyrenes containing cyanobiphenyl[22,23] as well as other mesogenic groups.[20,21] The decreasing trend implies a plasticization of the backbone by the side chain. It is tempting to suggest that the molecular origin of the alternation in T_g is the same as that for the clearing temperature. As we will see, odd-membered spacers allow for a more effective packing of the side chains and hence a decreased free volume when compared to an even-membered spacer. This would in turn be expected to increase the T_g of an odd member relative to that of an even member; a similar model has been used to rationalize the T_gs of liquid crystal copolymers.[34] Such an explanation, however, predicts that if the clearing temperatures exhibit an alternation, then so should the T_gs and this is not the case. Indeed,

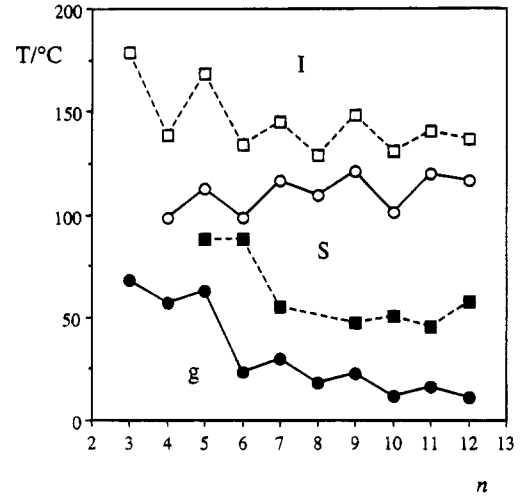

Figure 4. Dependence of the glass transition temperatures (●) and clearing temperatures (○) on the number n of methylene groups in the spacer for the poly[ω-(4′-cyanobiphenyl-4-yloxy)alkyl methacrylate]s. Also shown are the glass transition temperatures (■) and clearing temperatures (□) for the poly[ω-(4′-methoxybiphenyl-4-yloxy)alkyl methacrylate]s.[25] I, isotropic phase; S, smectic phase; g, glass phase.

while the observation of the odd–even effect is common for the clearing temperature, there are very few examples for which it observed for T_g. Thus, the molecular significance of the alternation in T_g is unclear. The clearing temperatures exhibit a more pronounced alternation as the length and parity of n are varied (see Figure 4), with the odd members of the series exhibiting the higher values. Such behavior can be rationalized by considering the alternation in the average shape of the side chain as the parity of the spacer is varied and its effect on the relative orientations of the mesogenic groups.[20,25] Thus for odd members, the mesogenic unit is orthogonal with respect to the backbone not only for the *all-trans* conformation of the spacer but also for selected conformations involving a single *gauche* defect. These arrangements maximize the interactions between the mesogenic groups and so result in higher transition temperatures. By contrast, such conformations do not exist for an even-membered spacer and the mesogenic units are constrained to lie at some angle with respect to the backbone. This prevents the mesogens from packing as efficiently and reduces the clearing temperature.

The dependence of the entropy change associated with the clearing transition, expressed as the dimensionless quantity $\Delta S/R$, on the number of methylene units in the spacer for the PMA-n series is shown in Figure 5. The overall trend in $\Delta S/R$ is an increasing one with increasing n and the small odd–even effect apparent initially is rapidly attenuated. These observations are in accord with the rationalization proposed to explain the dependence of the clearing temperatures on n[20,25] and may be accounted for by changes in the conformational component of the clearing entropy as n is varied. Thus, for an odd-membered spacer the liquid crystalline environment selects conformations which maintain the orthogonality of the mesogenic groups with respect to the backbone, giving rise to a greater conformational component in the overall entropy. On increasing the chain length, the number of conformers increases rapidly and this effect diminishes. Hence, the alternation in clearing entropies is attenuated on increasing n.

Figures 4 and 5 also show the analogous data for the

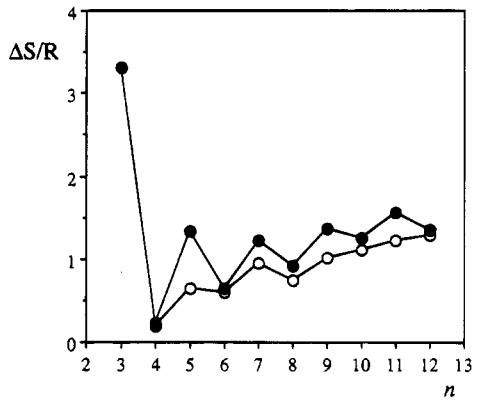

Figure 5. Dependence of the entropy change associated with the clearing transition (○) on the number n of methylene groups in the spacer for the poly[ω-(4′-cyanobiphenyl-4-yloxy)-alkyl methacrylate]s. Also shown are the clearing entropies (●) for the poly[ω-(4′-methoxybiphenyl-4-yloxy)alkyl methacrylate]s.[25]

poly[ω-(4′-methoxybiphenyl-4-yloxy)alkyl methacrylate]s, **4**.[25]

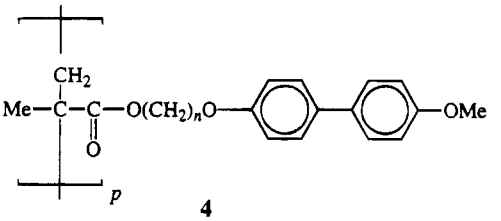

4

The glass transition temperatures of the methoxybiphenyl-substituted materials are on average *ca.* 37 °C higher than that exhibited by the corresponding cyanobiphenyl-substituted material; see Figure 4. The odd–even effect exhibited by the T_gs of series **1** as the length and parity of the spacer are varied is not seen for series **4**. By contrast, the alternation exhibited by the clearing temperatures of series **4** as n is varied is more pronounced than that observed for the cyanobiphenyl-based polymers, **1**. As with the glass transition temperatures, the clearing temperatures of series **4** are considerably higher, *ca.* 31 °C, than the corresponding member of series **1**. This is a surprising result given that in low molar mass mesogens the cyano group is generally considered more effective, albeit marginally, in enhancing clearing temperatures than the methoxy group.[35] It is often assumed that these knowledge-based rules describing structure–property relationships in low molar mass systems can be extrapolated to side-chain liquid crystal polymers and the rationale for this is that the spacer decouples the mesogenic unit from the backbone which may then be considered in essence to be a low molar mass unit. For the polymer series **1** and **4** such an extrapolation is not valid and to understand why we must consider probable local structures for the smectic phases. Cyanobiphenyl-based polymers generally form partially interdigitated smectic phases[36] (see Figure 6a), and for members of series **1** this has been shown to be the case.[32] By comparison, the side chains in polymers containing methoxy-substituted mesogenic groups tend to overlap to a much greater extent[36] (see Figure 6b), giving rise to structures tending toward that of the S_{A1} phase. In Figure 6 the backbones have been shown as confined by the smectic field to lie between the smectic layers. In the alternative extreme arrangement, the backbones may be considered to be largely unaffected by the smectic field and thus reside in

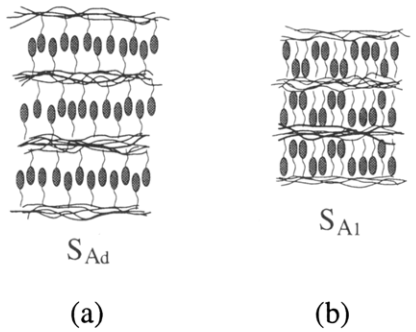

Figure 6. Schematic representations of (a) the partially interdigitated S_{Ad} phase and (b) the S_{A1} phase. Ellipses represent mesogenic groups.

essentially isotropic conformations.[36] For our purposes, however, it is the arrangement of the side chains which is of importance and not the backbones. It is clear from Figure 6 that the S_{A1} phase has a higher packing density than the S_{Ad} phase. Given the similar mesogenic tendencies of the two groups,[35] it is this more effective packing which gives rise to the higher clearing temperatures observed for series **4**. Also, for the S_{A1} phase the average shape of the side chain is more important given the more severe packing constraints. As we mentioned earlier, the average shape of the side chain is critically dependent on the parity of the spacer, and hence, for side-chain polymers exhibiting the S_{A1} phase a more pronounced alternation in clearing temperatures would be expected than for materials exhibiting the S_{Ad} phase for which the packing constraints are far less severe. Thus this difference in the local packing of the side chains allows for the higher clearing temperatures and the larger associated odd–even effect exhibited by the methoxybiphenyl-based polymers, **4**. This argument may be extended to consider the higher glass transition temperatures observed for series **4**. The S_{A1} phase possesses less free volume than the S_{Ad} phase, and hence, higher glass transition temperatures would be expected for the former, *i.e.* series **4**.

A comparison of the entropies associated with the clearing transition, expressed as the dimensionless quantity $\Delta S/R$, for series **1** and **4** is shown in Figure 5. The value of $\Delta S/R$ for the propyl member of series **4** is particularly high, and this polymer exhibits a crystal E–isotropic transition. The remaining transitions in both series are smectic A–isotropic transitions with the exception of the butyl member of series **4**, which is nematogenic. The entropy changes for **4** exhibit a more pronounced alternation than those for **1** as the length and parity of the spacer are varied; for both series the odd members show the higher values. In addition, the odd members of series **4** exhibit higher clearing entropies than the corresponding members of series **3**, whereas the even members of both series exhibit similar values of $\Delta S/R$. In the S_{A1} phase, the mesogenic unit overlaps the flexible spacer, and this interaction tends to order the spacer. Hence, at the smectic–isotropic transition this ordering effect should manifest itself as an increase in the conformational component of the clearing entropy. The odd-membered side chains can pack more effectively,[20,25] and hence this conformational contribution will be greater for odd rather than for even members. Thus, a more pronounced odd–even effect is observed for series **4** and the values of the clearing entropy are higher for the odd-members of series **4** than for the corresponding members of series **3**, see Figure 5.

Throughout this comparison of the thermal properties of series **3** and **4**, no reference has been made to the

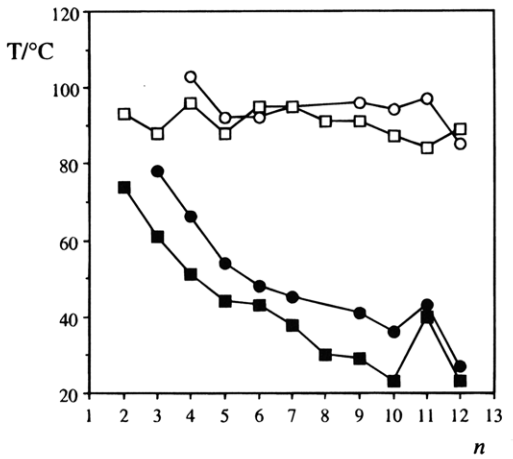

Figure 7. Dependence of the glass transition temperatures (●) and clearing temperatures (○) on the number n of methylene groups in the spacer for polynorbornene-based materials containing cyanobiphenyl.[18] Also shown are the glass transition temperatures (■) and clearing temperatures (□) for the analogous polymers containing methoxybiphenyl.[16,17]

nature of the polymer backbone. It is tempting to suggest, therefore, that these arguments should be valid for all backbones containing these or similar mesogenic units. As we indicated in the Introduction, there exist very few studies on complete homologous series of side-chain liquid crystal polymers and, in fact, there is just one other reported system for which such a complete data set exists, the polynorbornene-based materials, **5**, prepared by Schrock and his co-workers.[16–18]

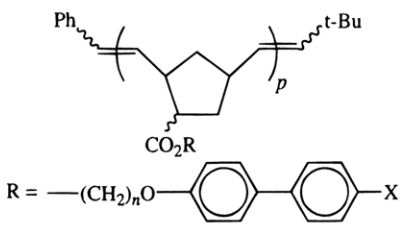

X = CN or OMe

5

The dependence of the glass transition temperatures and clearing temperatures of **5** with X = CN or OMe on the length of the flexible spacer n is shown in Figure 7. The glass transition temperatures for both sets of polymers decrease without alternation on increasing n and the cyanobiphenyl-based materials exhibit the higher values. The clearing temperatures of the cyanobiphenyl-based polymers are also generally higher than those of the methoxybiphenyl-substituted materials. These observations are contrary to the behavior shown in Figure 4. Figure 8 shows the dependence of the entropy change associated with the clearing transition for the two sets of polymer **5** and the cyanobiphenyl-based polymers exhibit slightly higher values. This result is particularly surprising for the dodecyl homologues for which the entropy change associated with a nematic–isotropic transition exhibited by the cyanobiphenyl-based polymer is greater than that for the smectic–isotropic transition exhibited by the methoxybiphenyl-substituted material. In general, therefore, the data shown in Figures 7 and 8 appear to contradict those shown in Figures 4 and 5. To explain this, the nature of the liquid crystal phases exhibited by these polymers must be considered: the polynorbornene-based materials are nematogens with the exception of the

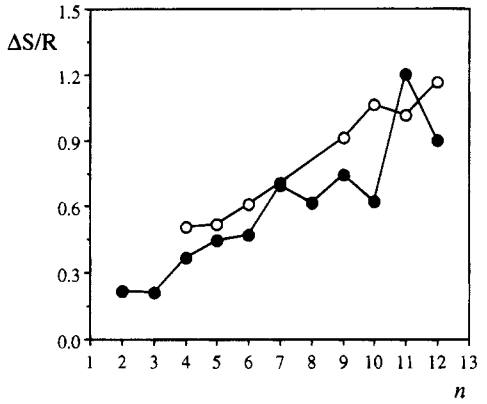

Figure 8. Dependence of the entropy change associated with the clearing transition on the number n of methylene groups in the spacer for polynorbornene-based materials containing cyanobiphenyl (○)[18] and methoxybiphenyl (●).[16,17]

undecyl and dodecyl members of the methoxybiphenyl series whereas the polymethacrylate-based materials are smectogens with the exception of the butyl member of series **4**. Thus, the rationalization of the behavior of series **1** and **4** in terms of the local arrangements of the side chains in the smectic phases would not be expected to hold for **5**. Furthermore, as there are no special steric considerations for the arrangement of the side chains in the nematic phase, it would be expected that the relative clearing temperatures of the side-chain polymers would reflect those of the analogous low molar mass mesogens and that only a small odd–even effect would be observed. These expectations are observed experimentally; see Figure 7.

We now turn our attention to the effect of backbone flexibility on the transitional behavior of side-chain liquid crystal polymers. Cyanobiphenyl was chosen as the mesogenic group for this study because it has been attached to a wide range of differing polymer backbones including polystyrene,[22,23] polynorbornene,[18] polyacrylate,[29–32,37–44] poly(vinyl ether),[7–15,45,46] and polysiloxane.[47–54] We have collated this data and extracted the data for the polymers having the highest reported molecular weights in each series. If the molecular weight data were not provided, then the polymer having the higher transition temperature was selected. The thermodynamic data were selected using the same criteria but for examples where such data were not provided for the highest molecular weight polymer, data relating to lower molecular weight materials have been used. This should not greatly affect the observed trends because the enthalpies of transition exhibit only a moderate or essentially no molecular weight dependence.[16–18,23,55–58] Figure 9 shows the structures of the backbones to be compared together with the acronyms used to refer to them.

Figure 10 shows the dependence of the glass transition temperatures on the length of the spacer n for each of the backbone types. The polysiloxane-based materials (PSX-n) exhibit the lowest T_gs for all values of n. For small values of n the polystyrene (PS-n) materials tend to exhibit the highest T_gs, then the polynorbornenes (PNB-n), polymethacrylates (PMA-n), and finally, the polyacrylates (PA-n) and poly(vinyl ether)s (PVE-n) tend to exhibit similar values of T_g. This relative ordering is in approximate agreement with that exhibited by the parent homopolymers. As the spacer length is increased, the T_g order changes and for the undecyl homologue

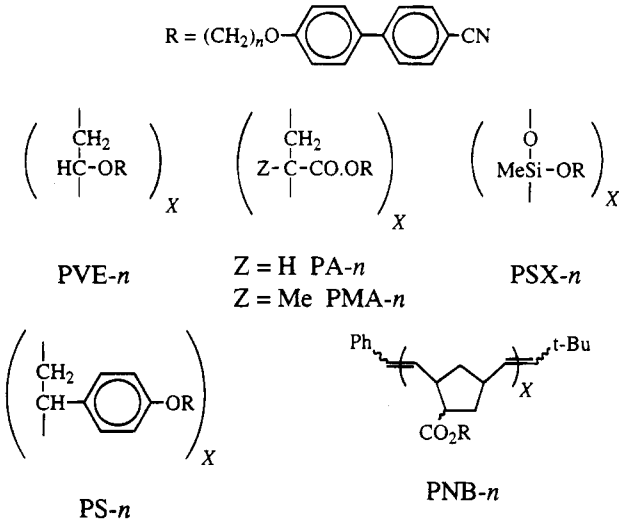

Figure 9. Structures of the polymers and corresponding acronyms: n refers to the number of methylene units in the spacer. PA, polyacrylate; PMA, polymethacrylate; PVE, poly(vinyl ether); PSX, polysiloxane; PS, polystyrene; PNB, polynorbornene.

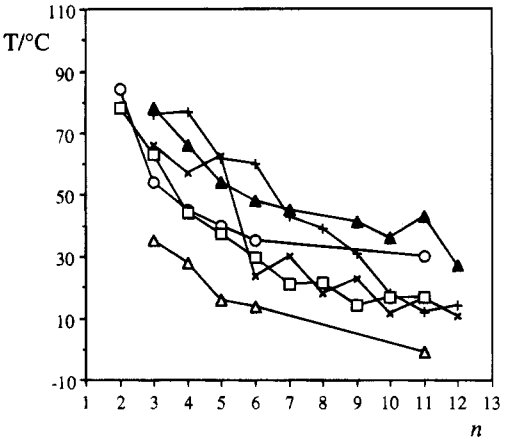

Figure 10. Glass transition temperatures for the PA-n (○), PMA-n (×), PVE-n (□), PSX-n (△), PS-n (+) and PNB-n (▲) series. n, is the number of methylene groups in the spacer. See Figure 9 for the meanings of the acronyms.

$$\text{PNB-11} > \text{PA-11} > \text{PVE-11} \approx \text{PMA-11} \approx \text{PS-11} > \text{PSX-11}$$

The T_gs for each series show a decreasing trend on increasing n resulting from the plasticization of the backbone by the side chains. The shapes of each T_g curve differ (see Figure 10), and this accounts for the change in the T_g order as n is increased. The T_gs of the PNB-n and PA-n series appear to reach a limiting value more quickly than those of the other series. The complex behavior shown in Figure 10 may, in part, be a result of comparing polymers some of whose properties may lie in the molecular weight dependent regime or be a result of specific end-group interactions. Further work is now required to establish these trends.

Figure 11 shows the dependence of the clearing temperatures on the length of the flexible spacer n for each series. This figure compares smectic–isotropic and nematic–isotropic transition temperatures; this is valid because it is generally found that for a given series in which a switchover from nematic to smectic behavior occurs, the alternation in the smectic–isotropic transition temperatures parallels that for the nematic–isotropic transition temperatures. Hence, the shape of the clearing curve does not depend, in general, on the types of transition being considered.[59] For small values

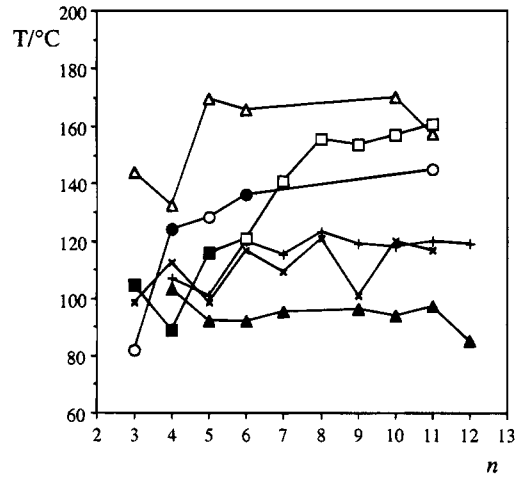

Figure 11. Clearing temperatures for the PA-*n* (S−I, ○; N−I, ●), PMA-*n* (S−I, ×) PVE-*n* (S−I, □; N−I, ■),PSX-*n* (S−I, △), PS-*n* (S−I, +) and PNB-*n* (N−I, ▲) series. *n* is the number of methylene groups in the spacer. See Figure 9 for the meanings of the acronyms.

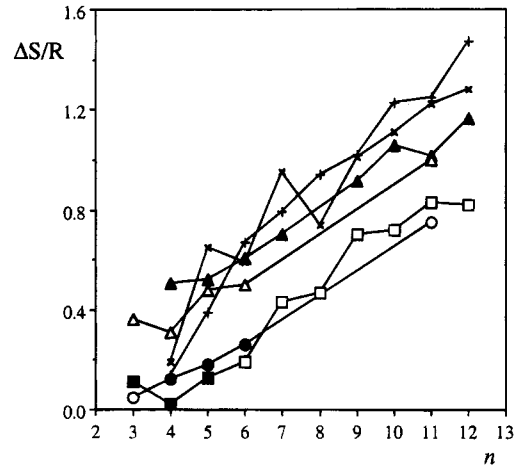

Figure 12. Clearing entropies for the PA-*n* (S−I, ○; N−I, ●), PMA-*n* (S−I, ×) PVE-*n* (S−I, □; N−I, ■),PSX-*n* (S−I, △), PS-*n* (S−I, +) and PNB-*n* (N−I, ▲) series. *n* is the number of methylene groups in the spacer. See Figure 9 for the meanings of the acronyms.

of *n* there is a complex dependence of the clearing temperature on backbone flexibility but as the spacer length increases, a general trend emerges that increasing the flexibility of the backbone enhances the clearing temperature. The clearing temperatures of the PNB-*n* series are lower than expected and we will return to this later.

Figure 12 shows the dependence of the entropy change associated with the clearing transition on *n* for each series. The values for PA-5, PA-6, and PVE-5 represent combined smectic−nematic−isotropic transitions.[15,38] The clearing entropies for each backbone show an increasing trend as *n* is increased, a result in accord with increasing the length of a terminal alkyl chain in low molar mass mesogens.[60,61] A surprising feature of Figure 12 is the absence of pronounced steps in the curves coinciding with switchovers from nematic to smectic behavior within particular series. For small values of *n* no clear relationship emerges between backbone flexibility and $\Delta S/R$ but as *n* is increased, decreasing flexibility tends to increase $\Delta S/R$. The PSX-*n* series appears to be an exception to this rule. However, it must be remembered that like transitions may not be being compared in all cases. Thus, these data appear to confirm that, in general, decreasing backbone flexibility tends to increase the value of the clearing entropy and this relationship has been shown also for polymers containing differing mesogenic groups.[62,63] This inverse relationship between backbone flexibility and $\Delta S/R$ has been rationalized by Percec and Tomazos[4,63,64] in terms of the distribution of the backbones within the smectic phase. Within the framework of their model, the smectic field is considered sufficiently strong to confine a flexible backbone to lie between the smectic layers forming a microphase-separated morphology. By comparison, the field is insufficient to restrict a rigid backbone and instead this passes through the smectic layers. In doing so the backbone is forced to adopt more extended conformations. Hence, at the clearing transition there will be a greater change in the conformational distribution of a rigid backbone than for a flexible backbone. The generality of this view has still to be determined because the relationship between the flexibility of the backbone and the conformation it adopts in a mesophase has still to be fully established.[65,66] However, the existing data do indeed tend to support the model.[67]

The behavior of both the clearing temperatures and entropies exhibited by the PNB-*n* series is anomalous. The clearing temperatures are lower than expected on the basis of backbone flexibility while the clearing entropies are significantly higher than expected for nematic−isotropic transitions. The depression of the clearing temperatures may be attributed to the complex microstructure of the polynorbornene chains including *cis* and *trans* double bonds as well as head-to-head, head-to-tail, and tail-to-tail arrangements of the repeat units.[16] These microscopic irregularities would also account for the pronounced nematic tendencies of these polymers. In addition, the separation of the mesogenic side chains is greater for the polynorbornene materials than for the other backbones and this dilution effect would also reduce the clearing temperatures and promote nematic behavior. The molecular significance of the unusually high $\Delta S/R$ values is unclear and indeed the rationalization of the low clearing temperatures in terms of either a complex microstructure or simply dilution effects would predict a reduction in $\Delta S/R$. However a factor not yet considered is the geometry of the link that connects the side chain to the polymer backbone. It has been shown that for low molar mass materials the molecular geometry of the link between a terminal chain and the mesogenic group is important in determining $\Delta S/R$.[68] It is reasonable to assume that this may also hold true for the link between the side-chain and polymer in side-chain liquid crystal polymers. Further speculation on this matter must await the results of model calculations.

Conclusions

The synthesis and thermal properties of ten members of a polymethacrylate-based side-chain liquid crystal polymer series incorporating cyanobiphenyl as the mesogenic group have been reported. The glass transition temperatures decrease initially on increasing spacer length before reaching a limiting value; superimposed on this trend is a small but distinct odd−even effect, in which the odd members exhibit the higher values. The clearing temperatures exhibit a more pronounced odd−even effect as the spacer length is varied, again the odd members exhibit the higher values. The entropy change associated with the clearing transition also exhibits an odd−even effect initially but this is attenuated on increasing *n* further. This behavior may be understood

by considering the average shape of the side chain as the parity of the spacer is varied.

A comparison of the thermal properties of the cyanobiphenyl-based series reported here with the corresponding series containing methoxybiphenyl revealed that the structure–property relationships developed for low molar mass mesogens should only be applied to side-chain polymers with caution. Specifically, the methoxybiphenyl-based materials exhibit significantly higher clearing temperatures than the cyanobiphenyl-based polymers. This surprising result is rationalized in terms of the probable local packing arrangements in the mesophase. By comparison, nematogenic polymer series appear to adhere more closely to the relationships developed for low molar mass mesogens.

The thermal properties of the PMA-*n* series are consistent with the general rule that increasing backbone flexibility for a given mesogenic group and spacer length enhances the clearing temperature while decreasing the associated entropy change. Exceptions to this rule may be a result of molecular weight or specific end-group effects. However, the importance of the geometry of the link that connects the side chain to the backbone has yet to be fully investigated.

Acknowledgment. The University of Aberdeen Research Committee is gratefully acknowledged for the award of a studentship to A.A.C. and for an award to C.T.I. to purchase the PL-DSC.

References and Notes

(1) *Side Chain Liquid Crystal Polymers*; McArdle, C. B., Ed.; Blackie and Sons: Glasgow, 1989.
(2) Attard, G. S. *Trends Polym. Sci.* **1993**, *1*, 79.
(3) Percec, V.; Pugh, C. In *Side Chain Liquid Crystal Polymers*; McArdle, C. B., Ed.; Blackie and Sons: Glasgow, 1989; Chapter 3.
(4) Percec, V.; Tomazos, D. In *Comprehensive Polymer Science, First Supplement*; Aggarwal, S. L., Russo, S., Eds.; Pergamon Press: Oxford, 1992; Chapter 14.
(5) Bowry, C.; Bonnett, P. *Opt. Comput. Proc.* **1991**, *1*, 13.
(6) Möhlmann, G. R.; van der Vorst, C. P. J. M. In *Side Chain Liquid Crystal Polymers*; McArdle, C. B., Ed.; Blackie and Sons: Glasgow, 1989; Chapter 12.
(7) Jonsson, H.; Sundell, P.-E.; Percec, V.; Gedde, U. W.; Hult, A. *Polym. Bull.* **1991**, *25*, 649.
(8) Heroguez, V.; Schappacher, M.; Papon, E.; Deffieux, A. *Polym. Bull.* **1991**, *25*, 307.
(9) Percec, V.; Lee, M. *Macromolecules* **1991**, *24*, 4963.
(10) Percec, V.; Lee, M.; Jonsson, H. *J. Polym. Sci., Part A: Chem. Ed.* **1991**, *29*, 327.
(11) Percec, V.; Lee, M. *Macromolecules* **1991**, *24*, 1017.
(12) Percec, V.; Lee, M. *Polym. Bull. (Berlin)* **1991**, *25*, 131.
(13) Percec, V.; Lee, M. *Macromolecules* **1991**, *24*, 2780.
(14) Percec, V.; Lee, M. *Polymer* **1991**, *32*, 2862.
(15) Percec, V.; Lee, M.; Ackerman, C. *Polymer* **1992**, *33*, 703.
(16) Komiya, Z.; Pugh, C.; Schrock, R. R. *Macromolecules* **1992**, *25*, 3609.
(17) Komiya, Z.; Pugh, C.; Schrock, R. R. *Macromolecules* **1992**, *25*, 6586.
(18) Komiya, Z.; Schrock, R. R. *Macromolecules* **1993**, *26*, 1393.
(19) Attard, G. S.; Dave, J. S.; Wallington, A.; Imrie, C. T.; Karasz, F. E. *Makromol. Chem.* **1991**, *192*, 1495.
(20) Imrie, C. T.; Karasz, F. E.; Attard, G. S. *Macromolecules* **1992**, *25*, 1278.
(21) Imrie, C. T.; Karasz, F. E.; Attard, G. S. *Macromolecules* **1993**, *26*, 545.
(22) Imrie, C. T.; Karasz, F. E.; Attard, G. S. *Macromolecules* **1993**, *26*, 3803.
(23) Imrie, C. T.; Karasz, F. E.; Attard, G. S. *J. Macromol. Sci., Pure Appl. Chem.* **1994**, *A31*, 1221.
(24) Imrie, C. T.; Karasz, F. E.; Attard, G. S. *Macromolecules* **1994**, *27*, 1578.
(25) Craig, A. A.; Imrie, C. T. *J. Mater. Chem.* **1994**, *4*, 1705.
(26) Attard, G. S.; Imrie, C. T.; Karasz, F. E. *Chem. Mater.* **1992**, *4*, 1246.
(27) Nakano, T.; Hasegawa, T.; Okamoto, Y. *Macromolecules* **1993**, *26*, 5494.
(28) Shannon, P. J. *Macromolecules* **1983**, *16*, 1677.
(29) Piskunov, M. V.; Kostromin, S. G.; Stroganov, L. B.; Shibaev, V. P.; Platé, N. A. *Makromol. Chem., Rapid Commun.* **1982**, *3*, 443.
(30) Kostromin, S. G.; Talroze, R. V.; Shibaev, V. P.; Platé, N. A. *Makromol. Chem., Rapid Commun.* **1982**, *3*, 803.
(31) Shibaev, V. P.; Kostromin, S. G.; Plate, N. A. *Eur. Polym. J.* **1982**, *18*, 651.
(32) Kostromin, S. G.; Sinitsyn, V. V.; Tal'roze, R. V.; Shibayev, V. P. *Polym. Sci. U.S.S.R.* **1984**, *26*, 370.
(33) Shibaev, V. P.; Platé, N. A. *Pure Appl. Chem.* **1985**, *57*, 1589.
(34) Schneider, H. A.; Percec, V.; Zheng, Q. *Polymer* **1993**, *34*, 2180.
(35) Gray, G. W. In *The Molecular Physics of Liquid Crystals*; Luckhurst, G. R., and Gray, G. W., Eds.; Academic Press: London, 1979; Chapter 1.
(36) Imrie, C. T.; Schleeh, T.; Karasz, F. E.; Attard, G. S. *Macromolecules* **1993**, *26*, 539.
(37) Bormuth, F. J.; Biradar, A. M.; Quotschalla, U.; Haase, W. *Liq. Cryst.* **1989**, *5*, 1549.
(38) Dubois, J.-C.; Decobert, G.; Le Barny, P.; Esselin, S.; Friedrich, C.; Noël, C. *Mol. Cryst. Liq. Cryst.* **1986**, *137*, 349.
(39) Kurihara, S.; Ikeda, T.; Tazuke, S. *Macromolecules* **1991**, *24*, 627.
(40) Le Barny, P.; Dubois, J.-C.; Friedrich, C.; Noël, C. *Polym. Bull. (Berlin)* **1986**, *15*, 341.
(41) Kostromin, S. G.; Shibaev, V. P.; Diele, S. *Makromol. Chem.* **1990**, *191*, 2521.
(42) Ikeda, T.; Kurihara, S.; Karanjit, D. B.; Tazuke, S. *Macromolecules* **1990**, *23*, 3938.
(43) Gubina, T. I.; Kise, S.; Kostromin, S. G.; Talroze, R. V.; Shibaev, V. P.; Plate, N. A. *Liq. Cryst.* **1989**, *4*, 197.
(44) Kurihara, S.; Ikeda, T.; Tazuke, S. *Macromolecules* **1993**, *26*, 1590.
(45) Sagane, T.; Lenz, R. W. *Macromolecules* **1989**, *22*, 3763.
(46) Kostromin, S. G.; Cuong, N. D.; Garina, E. S.; Shibaev, V. P. *Mol. Cryst. Liq. Cryst.* **1990**, *193*, 177.
(47) Kalus, J.; Kostromin, S. G.; Shibaev, V. P.; Kunchenko, A. B.; Ostanevich, Y. M.; Svetogorsky, D. A. *Mol. Cryst. Liq. Cryst.* **1988**, *155*, 347.
(48) Hsu, C. S.; Percec, V. *Polym. Bull. (Berlin)* **1987**, *18*, 91.
(49) Hsu, C. S.; Rodriguez-Parada, J. M.; Percec, V. *J. Polym. Sci., Part A: Chem. Ed.* **1987**, *25*, 2425.
(50) Gemmell, P. A.; Gray, G. W.; Lacey, D. *Mol. Cryst. Liq. Cryst.* **1985**, *122*, 205.
(51) Ringsdorf, H.; Schneller, A. *Makromol. Chem., Rapid Commun.* **1982**, *3*, 557.
(52) Nestor, G. N.; White, M. S.; Gray, G. W.; Lacey, D.; Toyne, K. J. *Makromol. Chem.* **1987**, *188*, 2759.
(53) Krücke, B.; Schlossarek, M.; Zaschke, H. *Acta Polym.* **1988**, *39*, 607.
(54) Percec, V.; Lee, M. *J. Macromol. Sci., Chem.* **1991**, *A28*, 651.
(55) Percec, V.; Hahn, B. *Macromolecules* **1989**, *22*, 1588.
(56) Hahn, B.; Percec, V. *Macromolecules* **1987**, *20*, 2961.
(57) Hsu, C. S.; Percec, V. *Makromol. Chem., Rapid Commun.* **1987**, *8*, 331.
(58) Percec, V.; Tomazos, D.; Pugh, C. *Macromolecules* **1989**, *22*, 3259.
(59) Attard, G. S.; Date, R. W.; Imrie, C. T.; Luckhurst, G. R.; Roskilly, S. J.; Seddon, J. M.; Taylor, L. *Liq. Cryst.* **1994**, *16*, 529.
(60) Marzotko, D.; Demus, D. *Paramna* **1975**, *Suppl. 1*, 189.
(61) Imrie, C. T.; Taylor, L. *Liq. Cryst.* **1989**, *6*, 1.
(62) Percec, V.; Tomazos, D.; Willingham, R. A. *Polym. Bull. (Berlin)* **1989**, *22*, 199.
(63) Percec, V.; Tomazos, D. *Polymer* **1990**, *31*, 1658.
(64) Percec, V.; Tomazos, D. *Adv. Mater.* **1992**, *4*, 548.
(65) Davidson, P.; Levelut, A. M. *Liq. Cryst.* **1992**, *11*, 469.
(66) Noirez, L.; Davidson, P.; Schwarz, W.; Pépy, G. *Liq. Cryst.* **1994**, *16*, 1081.
(67) Noirez, L.; Keller, P.; Cotton, J. P. *Liq. Cryst.* **1995**, *18*, 129.
(68) Emerson, A. P. J.; Luckhurst, G. R. *Liq. Cryst.* **1991**, *10*, 861.

MA946142T